Supplementary Information

Engineering Valence-Mismatched Ti^{4+} into Fe-based Metal-organic-frameworks for enhanced Photocatalytic CO_2 Reduction

Rui Li[1], Xiang Xue[1], Minqi Wu[1], Xuan Zuo[1], Huilin Hu[1], Guangshan Zhou,[2] Wang Zhang[2*], Jun Pan[2*], Xiangliang Pan[1*]

[1]College of Environment, Zhejiang University of Technology, Hangzhou 310014, China

[2]College of Materials Science and Engineering, Zhejiang University of Technology, Hangzhou 310014, China

E-mail: zhangwang@zjut.edu.cn (Wang Zhang); panjun0123@zjut.edu.cn (Jun Pan), panxl@zjut.edu.cn (Xiangliang Pan)

Experimental sections

1. Materials

N, N-dimethylformamide (DMF, AR), sodium sulfate (Na_2SO_4, AR), alcohol (AR) and acetonitrile (MeCN, GR) were purchased from Sinopharm (Kunshan, China). Ferric chloride anhydrous ($FeCl_3$, AR), titanium tetraisopropanolate (TTIP) and tris(2,2'-bipyridine) chlororuthenium (II) hexahydrate (AR) were purchased from Aladdin (Shanghai, China). 2-aminoterephthalic acid (NH_2-BDC) (AR) was purchased from Macklin (Fuzhou, China). Triethanolamine (TEOA, AR) was purchased from Meryer (Shanghai, China). All of the reagents were used as received without further purification or treatment.

2. Synthesize of photocatalysts

2.1. Synthesize of MIL-53-NH_2(Fe).

Fe-MIL-53-NH_2 was synthesized by a traditional solvent thermal method. 1.63 g (10 mmol) of $FeCl_3$ and 2.72 g (15 mmol) NH_2-BDC were dissolved in 20 mL and 30 mL of N, N-dimethylformamide (DMF), respectively. Then, the above two solutions were mixed completely through ultrasonic treatment. The mixed solution was put into a 100 mL Teflon-lined stainless-steel autoclave and stirred at 600 r/min for 30 minutes. After stirring, the solution was injected argon gas for 10 minutes, then placed in a 150 ℃ oven for 24 hours. After the reaction was completed, the catalysts were collected by centrifugation, washed twice with DMF and ethanol, and then dried by freeze-drying.

2.2. Synthesize of Ti ions doped MIL-53-NH_2(Fe)

The synthesis process of Ti doped Fe-MIL-53-NH_2 was the same as that of Fe-MIL-53-NH_2, except that the solution containing Fe ions is replaced with a solution containing

Ti/Fe ions at a certain molar ratio with the same concentration of metal ions. The molar ratio of Ti ions/Fe ions were 0.1/99.9, 0.5/99.5, 1/99 and 2/98, respectively.

3. Standard characterization

The crystal structure of Fe-MIL-53-NH_2 and Ti ions doped Fe-MIL-53-NH_2 were determined by using powder X-ray diffraction (PXRD, DX-27mini). The morphology of the catalysts can be observed through scanning electron microscopy (SEM, Nova Nano 450) and transmission electron microscopy (TEM, Talos S-FEG). Photoelectrochemical testing was conducted on the catalysts on an electrochemical workstation (CHI660E, Shanghai Chenhua Device Company, China). The valence band and chemical composition of elements in the catalysts were determined by X-ray photoelectron spectroscopy (XPS). The UV−vis diffuse reflectance spectra of the catalysts were determined by using a Shimadzu UV-2700. The recombination rate of photogenerated electron-hole pairs in the photocatalysts were measured using the photoluminescence (PL) spectrum (Hitachi F-4700). The *c*oncentration of Ti and Fe ions were measured by an inductively coupled plasma optical emission spectrometer (ICP-OES).

4. Electrochemical measurements

Photocurrent, electrochemical impedance spectroscopy (EIS), and Mott-Schottky (M-S) plot were measured by the electrochemical methods using an electrochemical workstation (CHI 660E). 4 mg of photocatalyst were dispersed in a mixture solution of 1 mL of ethanol and 100 μL of 5% Nafion solution. After 30 minutes of ultrasound, 100 μL of above solution were dropped onto the 1×1 cm^2 region of a 1×2 cm^2 Fluorine doped tin oxide glass (FTO) to prepare the working electrode. In the three electrode-measurement system, a Pt plate and an Ag/AgCl electrode were used as a counter electrode and a

reference electrode, respectively. 0.1 M Na_2SO_4 was used as electrolyte. The electrolyte was bubbled with N_2 for 15 minutes before using. An of 300 W Xe lamp (PLS-SXE300, Perfect Light Company, Beijing China)) with an AM 1.5 filter (1000 W m^{-2}) was employed as a light source. The test voltage was set to 0.5 V vs. Ag/AgCl. The EIS measurements were measured in the frequency range of 10^{-2} to 10^5 Hz. The Mott-Schottky measurements were measured at frequencies of 1000, 1500 and 2000, respectively.

5. Photocatalytic activity evaluation

The photocatalytic CO_2 reduction experiments were conducted in a 400 mL top-irradiation sealed quartz reactor with cooling water (Perfect, PQ256, Beijing). The photocatalytic system contains 5 mg MOFs as a photocatalyst, 40 mL of MeCN and 0.4 mL of H_2O as a solvent, 20 mg of tris(2,2'-bipyridine) chlororuthenium (II) hexahydrate as a photosensitizer, and 1 mL of TEOA as a sacrificial agent. An of 300 W Xe lamp (PLS-SXE300, Perfect Light Company, Beijing China)) with AM 1.5 filter/UVCUT420 filter/BP550 filter were used as the light sources. Before light irradiation, the reactor was filled with high purity CO_2 and then sealed. During photocatalytic reaction, the solution was continuously stirred. The photocatalytic products were analysed by gas chromatography equipped with a TCD detector and two FID detector (GC2014C, Shimadzu). Hydrogen, oxygen and nitrogen are detected through the TCD detector. CO, CH_4, C_2H_4, C_2H_6, C_2H_2 can be detected through FID detector.

The method of apparent quantum yield is based on the following equation (AQE) (1). The experimental conditions were consistent with the above photocatalytic CO_2 reduction conditions, except for the irradiation light source. A monochromatic light with a wavelength

of 550 nm was used for illumination. The light intensity measured using a light intensity meter is 0.081 $W \cdot cm^{-2}$. The illumination area is 56.14 cm^2.

$$AQE(\%)=N_e/N_p\times100\%=[2\times N_{CO}]/[(I\times A\times t)/(E_p\times N_A)]\times100\%$$

$$=[2\times N_{CO}]/[(I\times A\times t\times\lambda)/(hc\times N_A)]\times100\%$$

Where N_e represents the total number of electron transfers in the reaction, N_p represents the number of incident photons, N_{CO} represents amount of produced CO (mol), I, A and t represent power density ($W \cdot cm^{-2}$), light irradiation area (cm^2) and irradiation time (s), respectively, h is Planck's constant (6.62×10^{-34} J·s), c is speed of light (3.0×10^8 $m \cdot s^{-1}$), and λ is the monochromatic wavelength (550 nm).

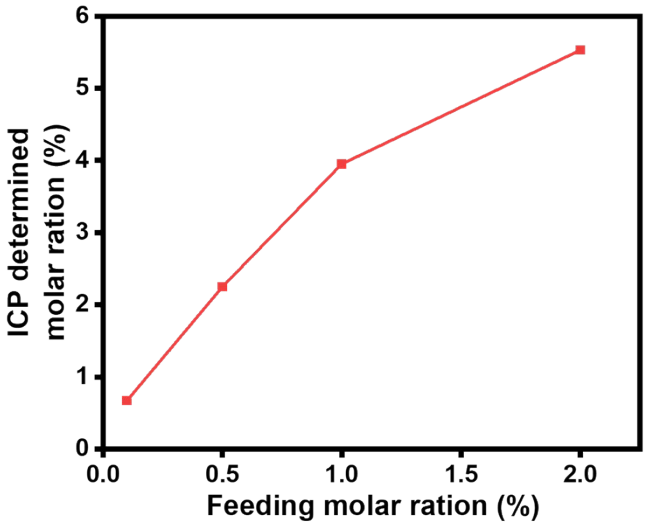

Fig. S1. The molar ratio of doping metals in Fe_x/Ti_y-MIL-NH_2 determined by ICP-OES.

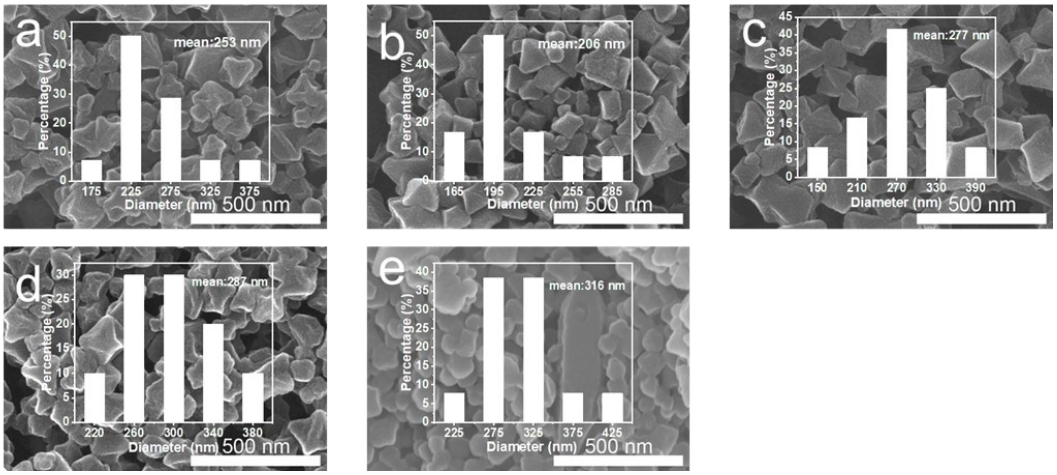

Fig. S2. SEM images and particle size analysis of (a) Fe-MIL-53-NH_2, (b) $Fe_{99.3}/Ti_{0.7}$-MIL-NH_2, (c) $Fe_{97.7}/Ti_{2.3}$-MIL-NH_2, (d) $Fe_{96.6}/Ti_{3.4}$-MIL-NH_2 and (e) $Fe_{94.5}/Ti_{5.5}$-MIL-NH_2.

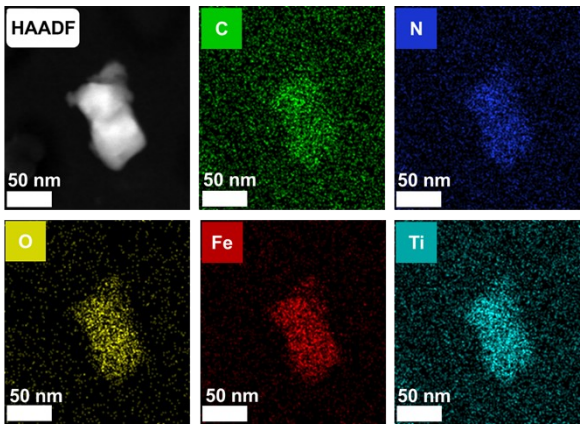

Fig. S3. The dark-field STEM image and corresponding elemental mapping of $Fe_{97.5}/Ti_{2.3}$-MIL-NH_2, showing the distribution of the C, N, O, Fe, and Ti elements. XPS spectra of $Fe_{97.7/}Ti_{2.3}$-MIL-NH_2.

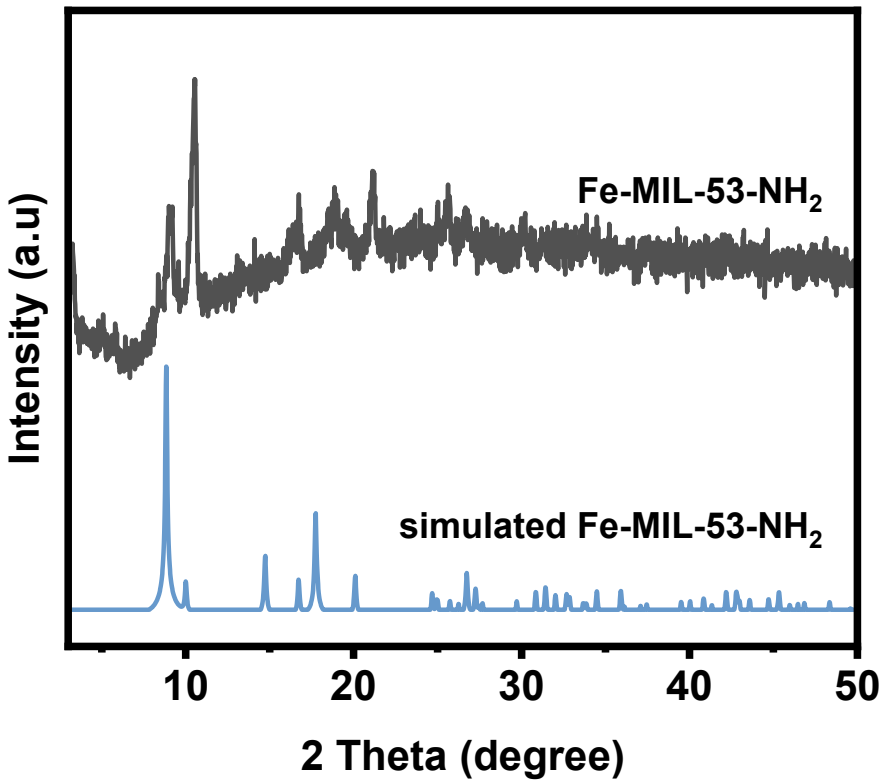

Fig. S4. XRD of Fe-MIL-53-NH_2.

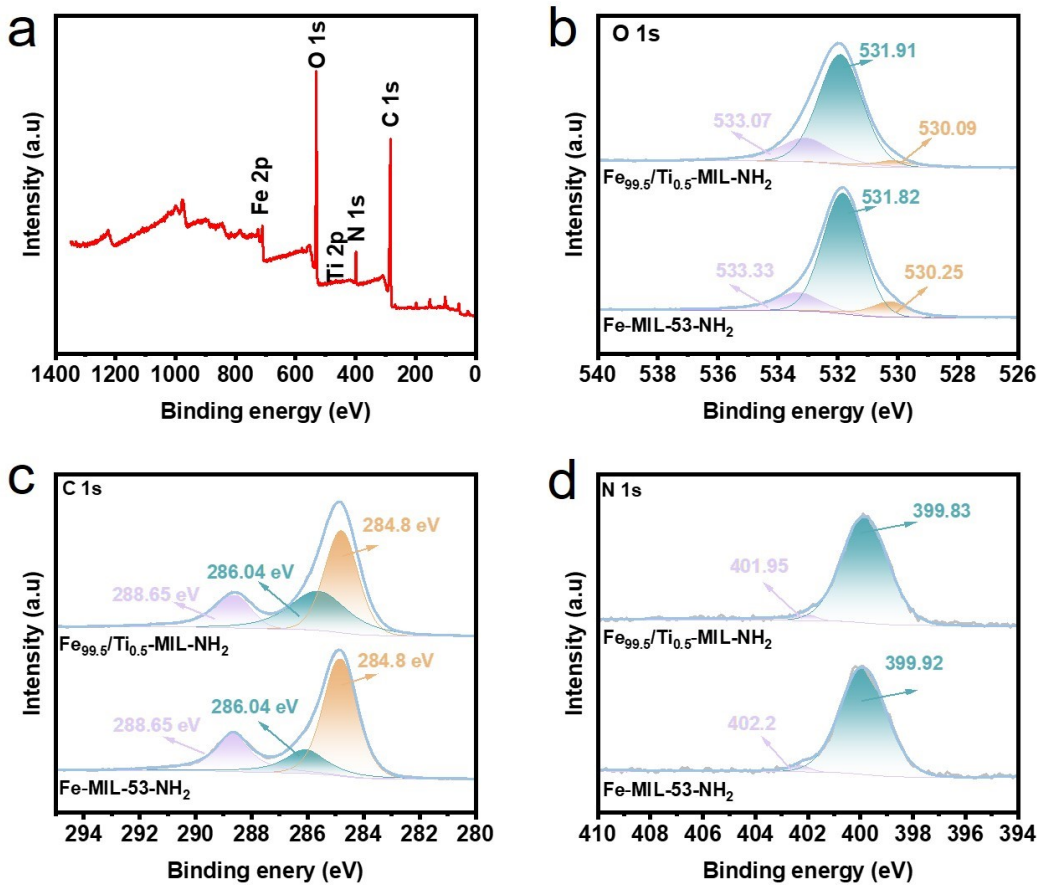

Fig. S5. The high-resolution XPS spectra of (a) survey scan, (b) C 1s, (c) O 1s and (d) N 1s of Fe-MIL-53-NH_2 and $Fe_{97.7}/Ti_{2.3}$-MIL-NH_2.

As showed in figure S5b showed the high-resolution O 1s spectra of $Fe_{97.7}/Ti_{2.3}$-MIL-NH_2, which has three characteristic peaks at 533.07, 531.91 and 530.09 eV, correspond to -O-C=O and hydroxy species, respectively [S-1]. In figure S5c, the C 1s high-resolution spectrum of $Fe_{97.7}/Ti_{2.3}$-MIL-NH_2 can be divided into three characteristic peaks at 288.65, 286.04 and 284.8 eV, which corresponding to C-N, C=C and C-C in phenyl, respectively[S-1].

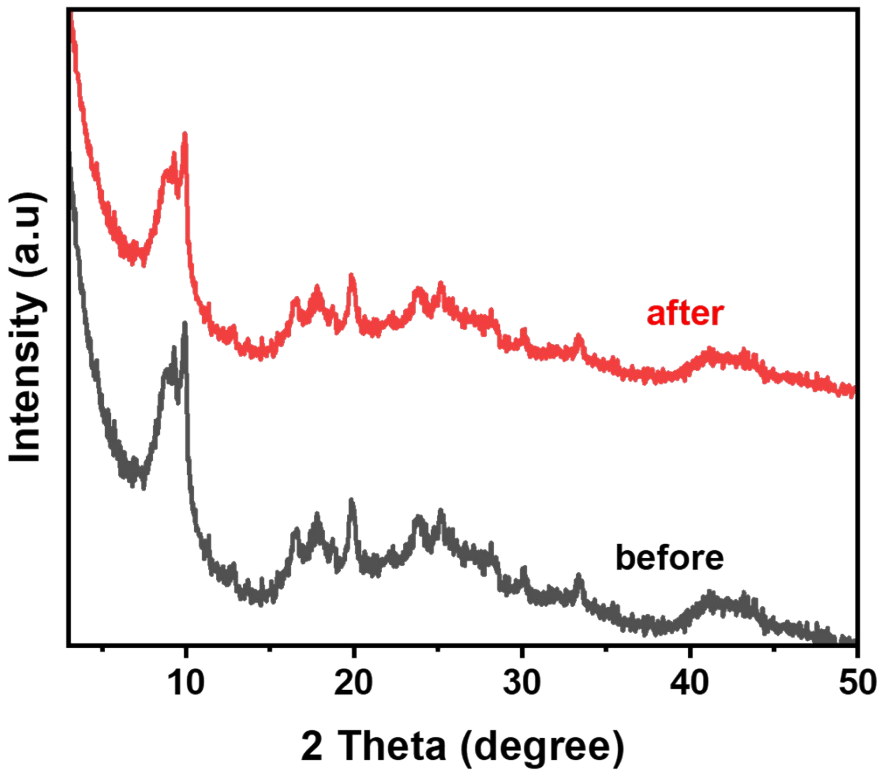

Fig. S6. XRD patterns of $Fe_{97.7}/Ti_{2.3}$-MIL-NH_2 before and after photocatalytic test.

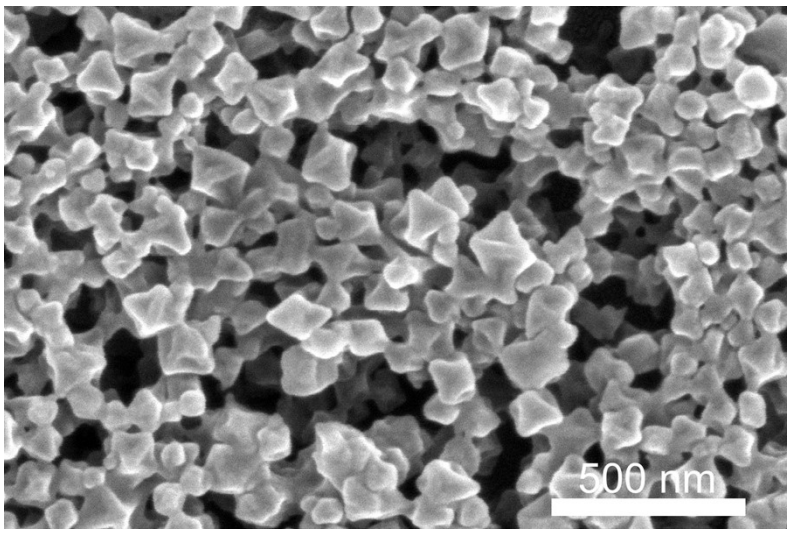

Fig. S7. SEM image of $Fe_{97.7}/Ti_{2.3}$-MIL-NH_2 after photocatalytic CO_2 reduction test.

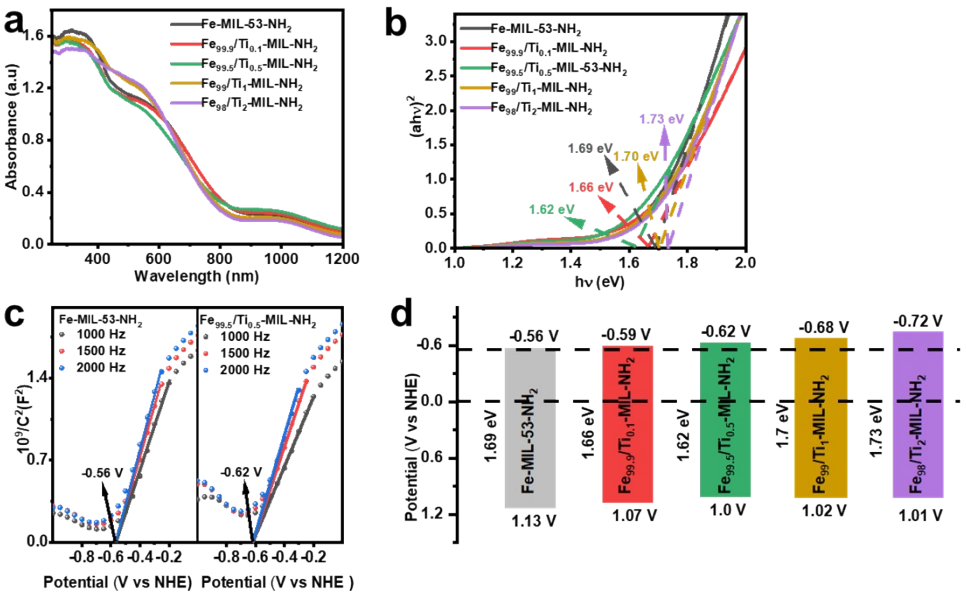

Fig. S8. (a) UV-vis spectra, (b) Tauc plots, (c) M-S plot and (d) energy band structures of synthesized samples.

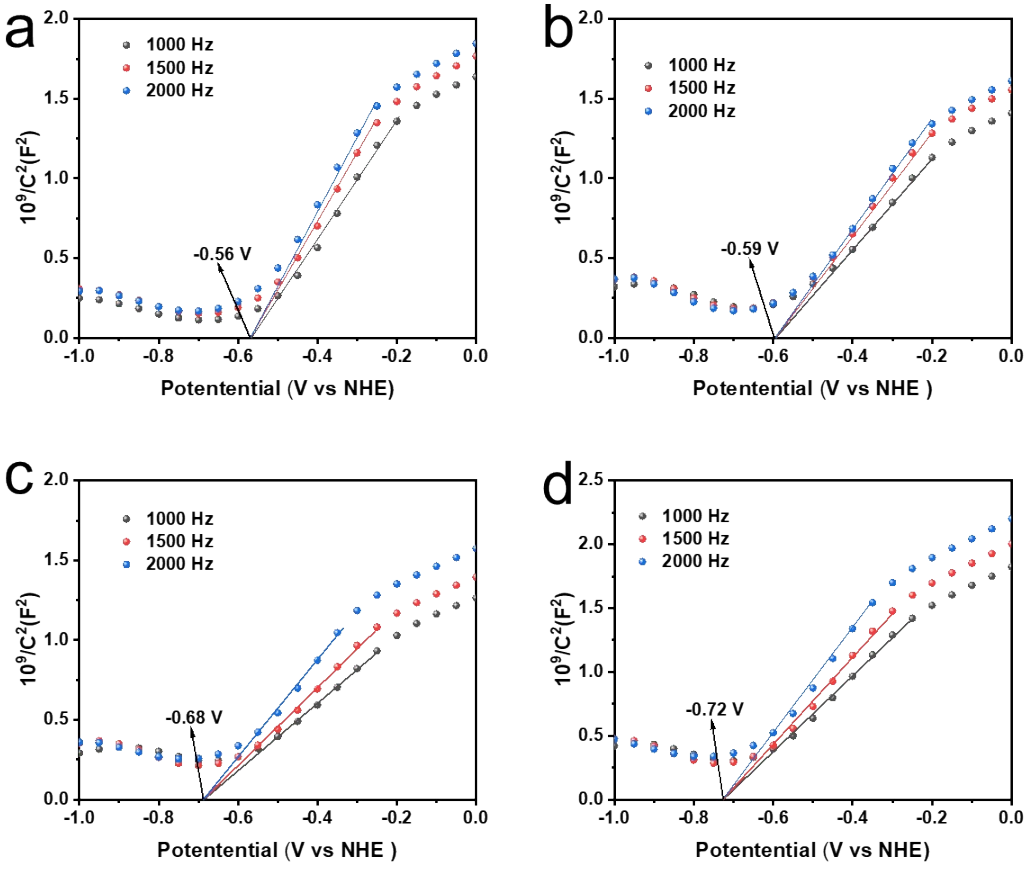

Fig. S9. Mott–Schottky curves of (a) Fe-MIL-53-NH_2, (b) $Fe_{99.3}/Ti_{0.7}$-MIL-NH_2, (c) $Fe_{96.6}/Ti_{3.4}$-MIL-NH_2 and (d) $Fe_{94.5}/Ti_{5.5}$-MIL-NH_2.

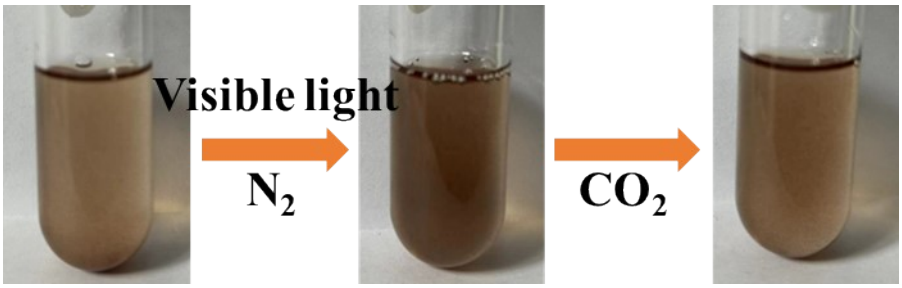

Fig. S10. Photographs of $Fe_{97.7}/Ti_{2.3}$-MIL-NH_2 in N_2 and CO_2 under visible light irradiation.

Table S1. The ion radius and electronegativities of Ti^{4+} and Fe^{3+}, as well as atomic numbers of Ti and Fe.

Metal ion	Radii(Å)	coordination number	atomic number	Ref.
Ti^{4+}	0.61	6	22	S-3, S-4
Fe^{3+}	0.64	6	26	S-5, S-6

Table S2. Ti and Fe concentrations and the molar ratios of Ti/Fe in metal ions doped MIL-53-NH_2.

Photocatalyst	ICP determined Fe concentration ($g \cdot g_{cat}^{-1}$)	ICP determined Ti concentration ($g \cdot g_{cat}^{-1}$)	ICP determined molar ration of Ti/(Fe+Ti)	Feeding molar ration of Ti/(Fe+Ti)
Fe-MIL-53-NH_2	0.0725	-	0	0
$Fe_{99.3}/Ti_{0.7}$-MIL-NH_2	0.0815	0.0005	0.0067	0.001
$Fe_{97.7}/Ti_{2.3}$-MIL-NH_2	0.0913	0.00177	0.0225	0.005
$Fe_{96.6}/Ti_{3.4}$-MIL-NH_2	0.0839	0.00284	0.0395	0.01
$Fe_{94.5}/Ti_{5.5}$-MIL-NH_2	0.0828	0.00393	0.0553	0.02

Table S3. Ration of Fe^{2+}/Fe^{3+} of Fe-MIL-53-NH_2 and $Fe_{99.5}Ti_{0.5}$-MIL-NH_2 of XPS

Photocatalyst	Area of Fe^{2+}	Area of Fe^{3+}	Ration of Fe^{2+}/Fe^{3+}
Fe-MIL-53-NH_2	10863	40809	0.45
$Fe_{97.7}/Ti_{2.3}$-MIL-NH_2	25621	18324	1.37

Table S4. Comparison of photocatalytic CO_2 reduction activity of Fe-based MOF photocatalysts .

Photocatalyst	Light source	Reaction conditions	Production	Ref.
NH_2-MIL-53(Fe)	>420 nm	50 mg photocatalyst MeCN=50 mL TEOA=10 mL	$HCOO^-$=46.5 μmol	S-7
Fe-MOF	>420 nm	0.5 mg photocatalyst MeCN=40 mL TEOA=10 mL H_2O=10 mL $[Ru(bpy)_3]Cl_2·6H_2O$=10 mg	CO=339.3 μmol g^{-1} h^{-1} CH_4=4.6 μmol g^{-1} h^{-1}	S-8
Fe-MOX	400-1000 nm	1 mg photocatalyst MeCN=3mL H_2O=2 mL TEOA=1 mL $[Ru(bpy)_3]Cl_2·6H_2O$=7.5 mg	CO=8 μmol g^{-1} h^{-1}	S-9
MIL-53 (Fe)	>420 nm	5 mg photocatalyst TEOA=2 mL H_2O=8 mL	CO=9 μmol g^{-1} CH_4=17 μmol g^{-1} h^{-1}	S-10
NH_2-MIL-101(Fe)	480-780 nm	5 mg photocatalyst MeCN=14 mL TEOA=1 mL	CO=21.3 μmol g^{-1} h^{-1}	S-11
MIL-88B(Fe)	>420 nm	5 mg photocatalyst H_2O=2 mL	CO=824 μmol g^{-1} h^{-1}	S-12
Dye/Co-Fe-MNS	>420 nm	5 mg photocatalyst MeCN=5 mL TEOA=1 mL $[Ru(bpy)_3]Cl_2$=20mg	CO=1637 μmol g^{-1} h^{-1}	S-13
50CN/Fe-MOF	>420 nm	30 mg photocatalyst H_2O=100 mL	CO=19.17 μmol g^{-1} h^{-1}	S-14
$Fe_{97.7}/Ti_{2.3}$-MIL-NH_2	>420 nm	5 mg photocatalyst MeCN=40 mL,H_2O=0.4 mL TEOA=1 mL $[Ru(bpy)_3]Cl_2·6H_2O$=20 mg	CO=7.24 mmol g^{-1} h^{-1}	This work

Table S5. Comparison of apparent quantum efficiency of Fe-based MOF photocatalysts

Photocatalyst	Wavelength (nm)	AQE (%)	Ref
MIL-88A	350	14.8	S15
50CN/Fe-MOF	300	0.18	S16
NH_2-MIL-101(Fe)@Bi_2MoO_6	450	0.09	S17
$Fe_{97.7}/Ti_{2.3}$-MIL-NH_2	550	0.82	This work

References

[S1] Z. Zhao, D. Yang, H. Ren, K. An, Y. Chen, Z. Zhou, W. Wang and Z. Jiang, *Chem. Eng. J*, 2020, **400**, 125929.

[S2] W. Xiong, Z. Zeng, X. Li, G. Zeng, R. Xiao, Z. Yang, H. Xu, H. Chen, J. Cao, C. Zhou and L. Qin, *Chemosphere*, 2019, **232**, 186-194.

[S3] Q. Luo, Y. Sun, J. Guo, J. Zhang and L. Fang, *J. Sol-Gel Sci. Technol.*, 2023, **106**, 158-172.

[S4] T. S. Sreena, P. P. Rao, A. K. V. Raj and T. R. A. Thara, *J. Solid State Chem.*, 2019, **278**, 120895.

[S5] D. Anbuselvan, S. Nilavazhagan, A. Santhanam, N. Chidhambaram, G. Kanimozhi, T. Ahamad and S. M. Alshehri, *J. Phys.: Condens. Matter*, 2021, **33**, 094001.

[S6] X. Wang, Z. Kang, D. Wang, Y. Zhao, X. Xiang, H. Shang and B. Zhang, *Nano Energy*, 2024, **121**, 109268.

[S7] D. Wang, R. Huang, W. Liu, D. Sun and Z. Li, *ACS Catal.*, 2014, **4**, 4254-4260.

[S8] W. Xu, G.-R. Zhang, J. Wang, H. Yu, W. Zhang, L.-L. Shen and D. Mei, *Adv. Funct.*

Mater., 2024, **34**, 2312691.

[S9] K. Yang, L. Chen, X. Duan, G. Song, J. Sun, A. Chen and X. Xie, *Ceram. Int.*, 2023, **49**, 16061-16069.

[S10] Y. Zhang, R. Huang, Y. Fang, J. Wang, Z. Yuan, X. Chen, W. Zhu, Y. Cai and X. Shi, *Sep. Purif. Technol.*, 2024, **336**, 126164.

[S11] N. Liu, K. Tang, D. Wang, F. Fei, H. Cui, F. Li, J. Lei, D. Crawshaw, X. Zhang and L. Tang, *Sep. Purif. Technol.*,2024, **332**, 125873.

[S12] F. Guo, R.-X. Li, S. Yang, X.-Y. Zhang, H. Yu, J. J. Urban and W.-Y. Sun, *Angew. Chemie. Int. Ed.*, 2023, **62**, 202216232.

[S13] A. Mahmoud Idris, X. Jiang, J. Tan, Z. Cai, X. Lou, J. Wang and Z. Li, *J. Colloid Interface Sci.*, 2022, **607**, 1180-1188.

[S14] X. Zhao, M. Xu, X. Song, W. Zhou, X. Liu and P. Huo, *Chinese. J. Catal.*, 2022, **43**, 2625-2636.

[S15] N. Ojha and S. Kumar, Appl. Catal. B: Environ, 2021, 292, 120166.

[S16] X. Zhao, M. Xu, X. Song, W. Zhou, X. Liu and P. Huo, Chin. J. Catal., 2022, 43, 2625-2636.

[S17] H. Feng, Y. Sun, Q. Xu and H. Liu, Appl. Catal. B: General, 2023, 664, 119350.